American Mineralogist, Volume 96, pages 1905–1908, 2011

LETTER

Murchisite, Cr_5S_6, a new mineral from the Murchison meteorite

CHI MA,* JOHN R. BECKETT, AND GEORGE R. ROSSMAN

Division of Geological and Planetary Sciences, California Institute of Technology, Pasadena, California 91125, U.S.A.

ABSTRACT

Murchisite (IMA 2010-003), Cr_5S_6, is a new chromium sulfide mineral, discovered in the Murchison CM2 meteorite. The type material occurs as one subhedral crystal (1.3 × 4 μm in size) in contact with low-Ni iron ("kamacite"), martensitic iron, schreibersite, and a Ca-,Al-rich glass, all of which are included in an isolated forsteritic olivine grain in the meteorite's matrix. The mean chemical composition determined by electron microprobe analysis of the type material is (wt%) Cr 53.32, S 42.87, V 1.44, Fe 1.14, P 0.10, Ni 0.10, sum 98.97. The empirical formula calculated on the basis of 6 S atoms is $(Cr_{4.60}V_{0.13}Fe_{0.09}Ni_{0.01})_{\Sigma 4.83}(S_{6.00}P_{0.01})_{\Sigma 6.01}$. Murchisite was also identified in another isolated olivine grain from the same meteorite. These crystals are subhedral to round in shape, 300 nm to 1 μm in size, and occur in association with tochilinite and serpentine, within which it is included, chromite, and eskolaite. Its electron backscatter diffraction patterns are an excellent match to that of synthetic Cr_5S_6 with the $P\bar{3}1c$ structure, showing a = 5.982, c = 11.509 Å, V = 356.67 Å^3, and Z = 2, based on previously published data from synthetic material. Murchisite is named for the locality (the Murchison meteorite). It is a low-temperature phase (~327 °C in the Cr-S system), probably formed from higher temperature $Cr_{1-x}S$ exsolved or expelled from a Cr-,S-bearing, metal-rich spherule included in forsteritic olivine grains that were probably derived from chondrule fragments. The formation of this phase reflects sulfur fugacities intermediate between those that would have led to troilite and those that would have led to no sulfide at all. The high-temperature $Cr_{1-x}S$ phase equilibrated with coexisting alloys to ~600 °C. Murchisite formed from this precursor at low temperatures (<~300 °C) through ordering of S vacancies.

Keywords: Murchisite, Cr_5S_6, new mineral, chromium sulfide, olivine, Murchison meteorite, carbonaceous chondrite

INTRODUCTION

During a nano-mineralogy investigation of the Murchison meteorite (a CM2), a new mineral, Cr_5S_6, was observed in two olivine grains. The Murchison meteorite, which fell near Murchison, Victoria, Australia, on September 28, 1969, is the most studied CM carbonaceous chondrite. High-resolution SEM, electron backscatter diffraction (EBSD), and electron microprobe analyses have been used to characterize its composition and structure. Synthetic Cr_5S_6 is well known in the field of materials science (Jellinek 1957; van Laar 1967) but has not been previously found in nature. This study reports the first natural occurrence of Cr_5S_6 and considers the origin of this phase, relationships to coexisting minerals, and implications through its formation and survival for the evolution of the host olivine and its constituents and of the alteration history of the Murchison meteorite.

MINERAL NAME AND TYPE MATERIAL

The new mineral and its name have been approved by the Commission on New Minerals, Nomenclature and Classification of the International Mineralogical Association (IMA 2010-003) (Ma 2010). The name murchisite is for the locality near which the meteorite was found. "Murchisite" has been selected for the name because the more natural choice, "murchisonite," was proposed as a mineral name by Levy (1827) and used during the nineteenth century as a synonym for orthoclase. Type material (Caltech Section MCM1B) has been deposited in the Smithsonian Institution's National Museum of Natural History, Washington, D.C., and is cataloged under USNM 7507.

OCCURRENCE, ASSOCIATED MINERALS, AND ORIGIN

One murchisite crystal (the type material) occurs with low-Ni iron ($Fe_{0.929}Ni_{0.060}P_{0.008}Co_{0.006}Cr_{0.003}$, formerly known by the now discredited name "kamacite"), martensitic iron ($Fe_{0.865}Ni_{0.124}P_{0.003}Co_{0.005}Cr_{0.004}$, a fine-grained alloy with a *bcc* α_2 structure), schreibersite ($Fe_{2.45}Ni_{0.55}P$) and a Ca-,Al-rich glass inside an isolated irregular olivine ($Fo_{99}Fa_1$) grain from the Murchison meteorite (Fig. 1). The olivine grain is exposed in one polished thick section, USNM 7507, prepared from a 1 cm^3 Murchison specimen at Caltech. This olivine grain is about 400 μm in size in the section plane, surrounded by a matrix of mostly fine-grained serpentine, olivine, and tochilinite [$6(Fe_{0.9}S)\cdot 5(Fe,Mg)(OH)_2$].

Murchisite is also observed in a second isolated olivine ($Fo_{99}Fa_1$) grain from Murchison in section MCM1A, occurring in mixtures of serpentine and tochilinite with chromite and eskolaite (Cr_2O_3) nearby (Fig. 2). Thin sections MCM1A and MCM1B are from adjacent slices of Murchison. In the meteorite (i.e., in 3D), the murchisite grains shown in Figures 1 and 2 were ~1 cm away from each other.

APPEARANCE, PHYSICAL AND OPTICAL PROPERTIES

The type material (1.3 × 4 μm in size) appears to be one subhedral crystal grain (Fig. 1) bounded by a native iron spherule

* E-mail: chi@gps.caltech.edu

and silicate glass. It is opaque in transmitted light and gray in reflected light. Streak, luster, hardness, tenacity, cleavage, fracture, optical properties, and density were not measured because of the small grain size. The density, calculated from the empirical formula, is 4.22 g/cm^3. The crystal is non-fluorescent under the beams of the electron microprobe and SEM. Murchisite in section MCM1A (Fig. 2) is subhedral to round in shape, 300 nm–1 μm in diameter. No forms or twinning were observed.

Chemical composition

Quantitative elemental microanalyses were conducted with a JEOL 8200 electron microprobe operated at 10 kV and 5 nA in a focused beam mode (150 nm nominal spot). Analyses were processed with the CITZAF correction procedure. Four individual analyses of the type material reported in Table 1 were carried out using WDS mode. The empirical formula, based on 6 S atoms, is $(Cr_{4.60}V_{0.13}Fe_{0.09}Ni_{0.01})_{\Sigma 4.83}(S_{6.00}P_{0.01})_{\Sigma 6.01}$. Portions of the Fe, P, and Ni contents might be from adjacent alloys and schreibersite. The end-member formula is Cr_5S_6, which requires Cr 57.47, S 42.53, total 100.00 wt%.

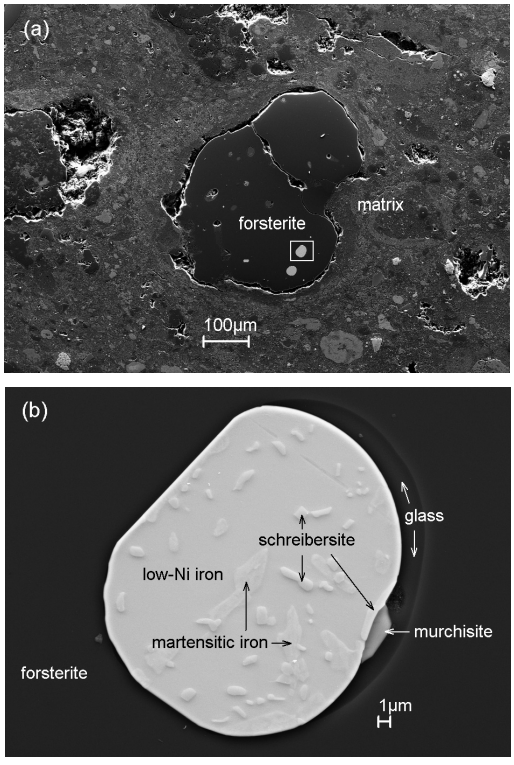

Figure 1. (**a**) Backscattered electron image of an isolated olivine grain in a Murchison section (USNM 7507); (**b**) enlarged BSE image showing murchisite (Cr_5S_6) with low-Ni iron, martensitic iron, schreibersite, and glass in a forsterite host.

Crystallography

Crystallography by EBSD at a sub-micrometer scale was carried out using methods described in Ma and Rossman (2009) with an HKL EBSD system on a ZEISS 1550VP scanning electron microscope operated at 20 kV and 6 nA in a focused beam with a 70° tilted stage. The structure was determined and cell constants were obtained by matching the observed EBSD pattern (Fig. 3) against the known structures of Cr_5S_6, Cr_7S_8, Cr_2S_3, CrS, brezinaite (Cr_3S_4) (Jellinek 1957; van Laar 1967), and daubréelite ($FeCr_2S_4$) (Raccah et al. 1966).

The EBSD patterns can be indexed nicely by the $P\bar{3}1c$ structure to give a best fit based on unit-cell data from synthetic Cr_5S_6 (Jellinek 1957) (Fig. 3). This yields a trigonal structure, space group: $P\bar{3}1c$, $a = 5.982$, $c = 11.509$ Å, $V = 356.67$ Å^3, and $Z = 2$ with mean angular deviations as low as 0.35. No errors are stated because the cell parameters are taken directly from the data of the matching phase in Jellinek (1957). The structure consists of close-packed S layers in hexagonal stacking with Cr in octahedral voids and ordered vacancies in every second interlayer (Jellinek 1957; van Laar 1967). The *c*:*a* ratio calculated from the unit-cell parameters is 1.924. The EBSD patterns of murchisite may also be indexed for most Kikuchi bands using the $P\bar{3}m1$ structure of synthetic Cr_7S_8, but this fails to account for some weak but readily visible bands like $(1\bar{5}\bar{2})$, $(5\bar{4}2)$, and $(14\bar{2})$ that can be indexed using the $P\bar{3}1c$ Cr_5S_6 structure.

X-ray powder-diffraction data (Cu$K\alpha_1$) are calculated from the cell parameters from Jellinek (1957) with the empirical formula of the type murchisite from this study using Powder Cell version 2.4 (2000). The strongest X-ray powder diffraction lines are [*d* in Å, (*I*), *hkl*] 4.724 (31) (101), 2.991 (59) (110), 2.654 (86) (112), 2.074 (100) (114), 1.727 (86) (300), 1.327 (20) (224), 1.105 (37) (308).

Origin and significance

Murchisite, as a new meteoritic chromium sulfide, joins the Cr-dominant meteoritic sulfide minerals brezinaite (Cr_3S_4) and daubréelite ($FeCr_2S_4$). The Murchison CM2 meteorite contains various phases with high-chromium contents including the oxides chromite and eskolaite and the new sulfide murchisite, all three

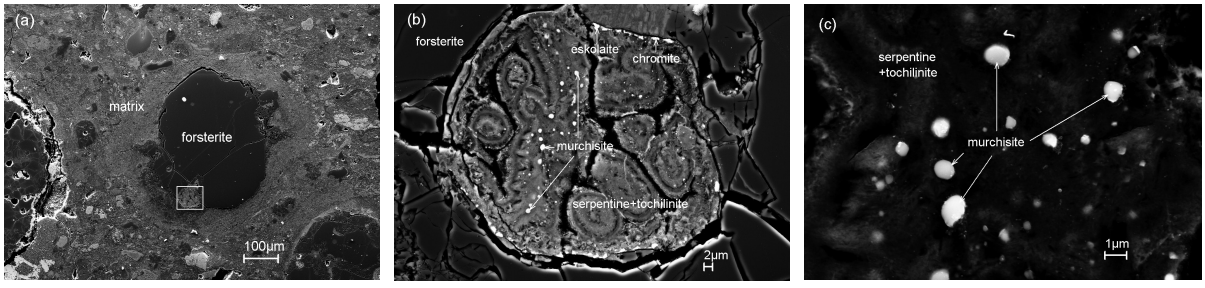

Figure 2. (**a**) BSE image of an isolated olivine grain in section MCM1A; (**b**) enlarged BSE image showing murchisite grains scattered in fine-grained serpentine and tochilinite with chromite and eskolaite at the edge of this altered inclusion; (**c**) further enlarged BSE image showing murchisite (bright grains).

TABLE 1. The mean electron microprobe analytical results for the type murchisite

Constituent	wt%	Range	SD	Probe standard
Cr	53.32	53.03–54.12	0.53	Cr metal
S	42.87	42.52–43.32	0.37	FeS_2
V	1.44	1.40–1.51	0.05	V metal
Fe	1.14	1.10–1.23	0.06	FeS_2
P	0.10	0.04–0.19	0.07	GaP
Ni	0.10	0.00–0.16	0.07	Ni metal
Total	98.97			

of which occur in MCM1A (Fig. 2).

A fundamental constraint on the origin of murchisite is its restricted thermal stability, limited in the Cr-S system, by a eutectoid at 297 °C with Cr_7S_8 and $Cr_{1-x}S$ and a peritectoid at 327 °C involving brezinaite and $Cr_{1-x}S$ (Venkatraman and Neumann 2006). The thermal stability of meteoritic murchisite may be enhanced by V and Fe relative to expectations based on the Cr-S system, but this is likely to be a modest effect as Fe, at least, is also relatively soluble in $Cr_{1-x}S$, the stable high-temperature phase for a Cr sulfide with murchisite's composition (Venkatraman and Neumann 2006). Murchisite formed at very low temperatures.

Murchisite may, in principle, form through either closed or open system reactions. Consider the type example (Fig. 1). The murchisite grain resides in an inclusion hosted by olivine that also contains the alloys low-Ni iron and martensitic iron, schreibersite, and glass. Alloys in CM chondrites are highly susceptible to oxidation/hydration where exposed to aqueous fluids (e.g., Rubin et al. 2007), but we see no evidence for tochilinite or serpentine. Moreover, neither the glass, which is readily serpentinized, nor the schreibersite, which is readily oxidized, are altered although alteration phases are present less than 100 μm away in the matrix. Inclusions in other forsteritic olivines from Murchison are often serpentinized (Fig. 2), so these features suggest that the host olivine successfully protected this inclusion from aqueous alteration. Given the low thermal stability of murchisite, it is unlikely that a low-temperature open system sulfidation event could account for the type sample because it would have to have occurred through one or more cracks that would not have healed prior to aqueous alteration. At the time the type murchisite grain formed, the system was closed.

Some context for the formation of murchisite can be gleaned from an analysis of the alloy-phosphide spherule that coexists with it by using phase relations of the system Fe-Ni-P. In Figure 4, we show Ni contents of the three coexisting phases schreibersite, low-Ni iron, and taenite from experimental data of Doan and Goldstein (1970) and Romig and Goldstein (1981) plotted as a function of temperature. From analyzed compositions of the meteoritic phases, large-scale multi-micrometer variations in chemistry within the metal spherule ceased around ~600 °C, consistent with rapid cooling and no significant reheating. Taenite, which has an fcc structure at high temperatures, undergoes a nearly diffusionless transformation to the bcc martensite structure at low temperatures (e.g., Kaufman and Olson 1958), and it is this martensite phase that we observe. Our EBSD measurements show only the bcc lines of martensitic iron, which implies that the martensitic iron never decomposed to plessite (mixture of taenite and low-Ni iron), again consistent with no significant reheating to temperatures above ~300 °C once quenched.

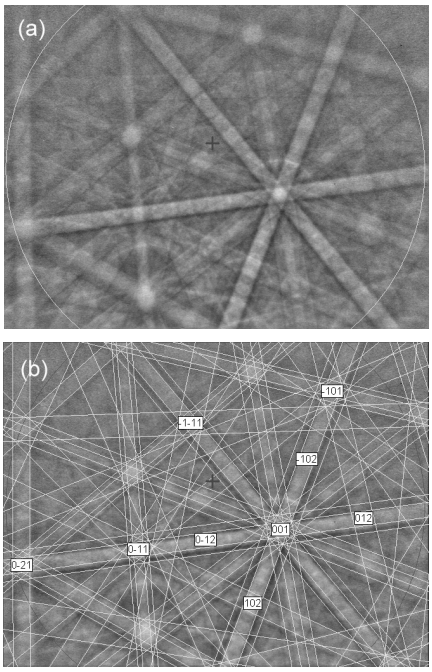

FIGURE 3. (**a**) EBSD pattern of a murchisite crystal; (**b**) the pattern indexed with the $P\bar{3}1c$ structure of synthetic Cr_5S_6.

It might be expected that a Cr-rich phase like murchisite is the consequence of an unusually high-Cr content in the original alloy but the observed wt% Cr is only 0.2–0.4, or slightly higher if all of the murchisite Cr is assumed to have originated from the alloy, and this range is at the low end of values reported in the literature for Murchison alloys (0.2–1.0 wt% Cr; Fuchs et al. 1973; Grossman and Olsen 1974). It seems more likely that S and not Cr was the component most critical to the formation of murchisite. In the type inclusion, the S_2 fugacity was too low to stabilize alloy-saturated troilite, pyrrhotite, pentlandite, or daubréelite but high enough to stabilize a Cr-rich monosulfide. Given the stabilization of daubréelite relative to alloy plus Cr-rich monosulfides with decreasing temperature (Jacob et al. 1979), the absence of daubréelite suggests that exposure time to temperatures between ~300 °C, below which kinetics of reaction between alloy and sulfide are likely too slow to form daubréelite, and ~600 °C, above which there is a stable Fe-rich alloy–Cr-rich monosulfide field, was relatively short. In contrast to the heterogeneous reaction required to form daubréelite, the transformation of $Cr_{1-x}S$ to murchisite requires only ordering of sulfur vacancies and this is rapid even at very low temperatures. These considerations are consistent with observations described above for the adjacent metal-phosphide spherule. We conclude that the precursor of murchisite was $Cr_{1-x}S$ formed through expulsion of a molten sulfide from alloy during chondrule formation or through later subsolidus exsolution from the alloy at temperatures at or above ~600 °C. This phase equilibrated with coexisting alloys during cooling to ~600 °C (cf. Fig. 4). The formation of $Cr_{1-x}S$ was nebular. In a planetary metamorphic environment capable of reaching ~600 °C, cooling would have been slow enough so that martensitic iron (e.g., Fig. 1b) would have broken down (e.g., Reisener and Goldstein 2003) and there would have been many signatures of high-temperature metamorphism in Murchison that are not observed. The presence of martensitic iron speaks to a rapid quench during chondrule formation to temperatures

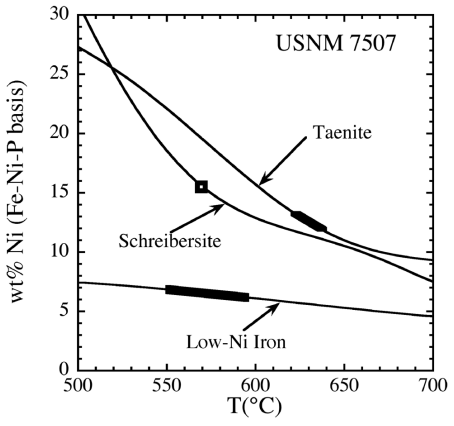

FIGURE 4. Weight percent Ni in coexisting low-Ni iron, taenite, and schreibersite in the system Fe-Ni-P as a function of temperature. Curves were constructed from isothermal phase diagrams of Doan and Goldstein (1970) and Romig and Goldstein (1981). Compositions of low-Ni iron, schreibersite, and martensitic iron shown in Figure 1b are plotted on the curves. This assumes that what is now martensitic iron was, at higher temperatures, taenite. Schreibersite analyses are mixtures of schreibersite and low-Ni iron. We assumed a formula of $(Fe,Ni,Cr,Co)_3P$ and estimated the phosphide composition by plotting molar Fe, Ni, Co, and Cr as a function of P, extrapolating linearly to 25 mol% P, and renormalizing to $(Fe,Ni)_3P$. Martensitic iron analyses are also likely contaminated by low-Ni iron, so plotted compositions on the taenite curve should be regarded as minimum values for Ni.

below ~300 °C, but just how fast a quench this was and whether it prevented the transformation of $Cr_{1-x}S$ to murchisite is unknown. It is therefore possible that the type murchisite formed from $Cr_{1-x}S$ in a nebular setting in its closed environment inside the host olivine or on the Murchison parent body in its closed environment inside the host olivine. Regardless of where the host olivine was at the time murchisite formed from $Cr_{1-x}S$, the type murchisite is a low-temperature manifestation of a high-temperature preplanetary (i.e., nebular) phase.

In the second murchisite occurrence (Fig. 2), murchisite forms a scattered band of small crystals within a mixture of tochilinite and serpentine included in forsteritic olivine. Eskolaite and chromite are restricted to the margins of the inclusion. Neither phosphides nor phosphates were observed. In contrast to the type example described above, this inclusion was exposed to an altering fluid that destroyed any original metal, pyroxenes, and/or glass, presumably either through a crack or because the inclusion was exposed directly to matrix in the third dimension.

Chromium can be soluble and, hence mobile, in acidic aqueous solutions, which could lead to dissolution of murchisite. However, for the high pHs pertinent to serpentinization of Murchison (e.g., Guo and Eiler 2007), Cr would have been relatively immobile. Thus, the Cr-rich phases observed in Figure 2 probably originated from Cr within the original inclusion as formed at high temperatures and in roughly the locations they are currently found in. Chromite can form near metal inclusion rims through oxidation during chondrule melting (Lauretta and Buseck 2003), but the presence of eskolaite and chromite at the margins of the inclusion in Figure 2b is also consistent with murchisite being exposed to alteration conditions that were oxidizing and basic relative to those needed to stabilize murchisite. If so, the alteration process did not proceed long enough to oxidize interior crystals of murchisite, perhaps due to armoring by tochilinite.

Given the close proximity of the two known occurrences of murchisite, it is highly likely that all of these grains formed as Cr monosulfides at relatively high temperature with later ordering of S vacancies at low temperatures, below ~300 °C, to form murchisite. Moreover, the fact that murchisite was not observed in other sections from the same ~1 cm^3 sample of murchisite or in sections from elsewhere in the meteorite suggests that the conditions necessary for the formation of murchisite are generally not met. A different sulfide (e.g., troilite) is produced if sulfur fugacities inside the inclusion are high enough, daubréelite would form if a $Cr_{1-x}S$ + alloy assemblage were held at temperatures below ~600 °C for an extended period of time, and there would be no sulfide at all if the sulfur fugacities were too low. Murchisite is a goldilocks phase.

ACKNOWLEDGMENTS

The Caltech Analytical Facility at the Division of Geological and Planetary Sciences is supported, in part, by Grant NSF EAR-0318518 and the MRSEC Program of the NSF under DMR-0080065. We thank Stuart Mills, Panagiotis Voudouris, Ian Swainson, and an anonymous reviewer for helpful reviews of the manuscript.

REFERENCES CITED

Doan, A.S. and Goldstein, J.I. (1970) The ternary phase diagram, Fe-Ni-P. Metallurgical Transactions, 1, 1759–1767.

Fuchs, L.H., Olsen, E., and Jensen, K.J. (1973) Mineralogy, mineral-chemistry, and composition of the Murchison (C2) meteorite. Smithsonian Contributions to the Earth Sciences, 10, 1–39.

Grossman, L. and Olsen, E. (1974) Origin of the high-temperature fraction of C2 chondrites. Geochimica et Cosmochimica Acta, 38, 173–187.

Guo, W. and Eiler, J.M. (2007) Temperatures of aqueous alteration and evidence for methane generation on the parent bodies of the CM chondrites. Geochimica et Cosmochimica Acta, 71, 5565–5575.

Jacob, K.T., Rao, D.B., and Nelson, H.G. (1979) Phase relations in the Fe-Ni-Cr-S system and the sulfidation of an austenitic stainless steel. Oxidation of Metals, 13, 25–55.

Jellinek, F. (1957) The structures of the chromium sulphides. Acta Crystallographica, 10, 620–628.

Kaufman, L. and Olson, M. (1958) Thermodynamics and kinetics of martensitic transformations. Progress in Metal Physics, 7, 165–246.

Lauretta, D.S. and Buseck, P.R. (2003) Opaque minerals in chondrules and fine-grained chondrule rims in the Bishunpur (LL3.1) chondrite. Meteoritics and Planetary Science, 38, 59–79.

Levy, A. (1827) On a new mineral substance proposed to be called Murchisonite. Philosophical Magazine, 1, 448–452.

Ma, C. (2010) Murchisite, IMA 2010-003. CNMNC Newsletter 2, April 2010, p. 377. Mineralogical Magazine, 74, 375–377.

Ma, C. and Rossman, G.R. (2009) Tistarite, Ti_2O_3, a new refractory mineral from the Allende meteorite. American Mineralogist, 94, 841–844.

Raccah, P.M., Bouchard, R.J., and Wold, A. (1966) Crystallographic study of chromium spinels. Journal of Applied Physics, 37, 1436–1437.

Reisener, R.J. and Goldstein, J.I. (2003) Ordinary chondrite metallography: Part 1. Fe-Ni taenite cooling experiments. Meteoritics and Planetary Science, 38, 1669–1678.

Romig, A.D. and Goldstein, J.I. (1981) Determination of the Fe-Ni and Fe-Ni-P phase diagrams at low temperatures (700 to 300 C). Metallurgical Transactions, 11A, 1151–1159.

Rubin, A.E., Trigo-Rodríguez, J.M., Huber, H., and Wasson, J.T. (2007) Progressive aqueous alteration of CM carbonaceous chondrites. Geochimica et Cosmochimica Acta, 71, 2361–2382.

van Laar, B. (1967) Ferrimagnetic and antiferromagnetic structures of Cr_5S_6. Physical Review, 156, 654–662.

Venkatraman, M. and Neumann, J.P. (2006) Cr-S phase diagram. ASM Alloy Phase Diagrams Center, P. Villars, editor-in-chief; http://www1.asminternational.org/AsmEnterprise/APD. ASM International, Materials Park, Ohio.

MANUSCRIPT RECEIVED APRIL 11, 2011
MANUSCRIPT ACCEPTED JULY 13, 2011
MANUSCRIPT HANDLED BY IAN SWAINSON